Transactions of NAMP 23, (2025) 69-76

Transactions of
The Nigerian Association of
Mathematical Physics
Journal homepage: https://nampjournals.org.ng

THEORETICAL PREDICTION OF INSTABILITY AND HALF-METALLICITY IN THE $NaCaO_3$ PEROVSKITE: A DFT APPROACH

[*1]OSUHOR, O. P. AND [2]NWACHUKU, D. N.

[1,2] *Department of Physics, University of Delta, Agbor, Delta State, Nigeria..*

ARTICLE INFO

Article history:
Received xxxxx
Revised xxxxx
Accepted xxxxx
Available online xxxxx

Keywords:
Perovskite,
Semiconductor,
Mechanical Properties,
Half-metallic,
Spintronic.

ABSTRACT

The structural, mechanical, electronic, and vibrational properties of the $NaCaO_3$ perovskite compound were examined using density functional theory (DFT) within the Quantum ESPRESSO software package. The calculations employed the plane-wave pseudopotential method. Mechanical analysis shows that the bulk-to-shear modulus ratio (B/G = 7.03) suggests ductile behavior, whereas the elastic stability criterion is not satisfied due to a negative value of C_{44} (–4.42 GPa), indicating that the structure is mechanically unstable. The electronic band structure further reveals that $NaCaO_3$ exhibits half-metallicity: the spin-up channel displays semiconducting features with a direct bandgap of 4.69 eV, while the spin-down channel demonstrates metallic behavior. The density of states (DOS) analysis indicates that the conduction band is primarily derived from Ca-4d orbitals, while the valence band is dominated by O-2p orbitals. These results provide important insights into the intrinsic properties of $NaCaO_3$, emphasizing its potential for spintronic and electronic applications. Nevertheless, additional investigations using alternative computational approaches are recommended to validate and complement these findings.

1. INTRODUCTION

Perovskite materials have recently gained prominence as a versatile class of compounds owing to their exceptional combination of electrical, dielectric, and magnetic properties, which make them promising candidates for a broad spectrum of advanced technological applications [1]. Their remarkable physical and chemical characteristics have attracted significant attention, positioning them as leading materials for solar cells, optoelectronics, energy conversion, protective coatings, and contemporary electronic devices [2]. Defined by the general formula ABX_3, perovskites represent one of the most extensively studied crystalline systems in condensed matter physics and materials science. The ideal perovskite lattice consists of a cubic framework where the A-site cation occupies the central position in 12-fold coordination, the B-site cation resides at the corners in 6-fold octahedral coordination, and the X-site anions occupy the face-centered positions.

[*]Corresponding author: OSUHOR, O. P.
E-mail address: o.osuhor@unidel.edu.ng
https://doi.org/10.60787/tnamp.v23.626

This structural configuration permits extensive compositional flexibility, thereby enabling tunable properties suitable for applications ranging from superconductivity and ferroelectricity to photovoltaics and spintronics [3].

The diverse physical behavior of perovskites underscores their scientific and technological significance. For instance, oxide perovskites such as $BaTiO_3$ exhibit ferroelectric properties, while compounds like $Ba_2YCu_3O_7$ display superconductivity. Their technological importance also stems from their ability to demonstrate both ionic and electronic conductivity, coupled with their effectiveness as catalysts for a variety of reactions [4]. This versatility has expanded their use across multiple fields of modern technology. Double perovskites, for example, are recognized for their half-metallic nature, making them suitable for spin injection and tunneling magnetoresistance devices [5]. Meanwhile, halide perovskites have revolutionized photovoltaic research, achieving laboratory power conversion efficiencies exceeding 30% while maintaining advantages such as low fabrication cost, solution-processability, and tunable band gaps [6].

Crystallographic Structure of $NaCaO_3$

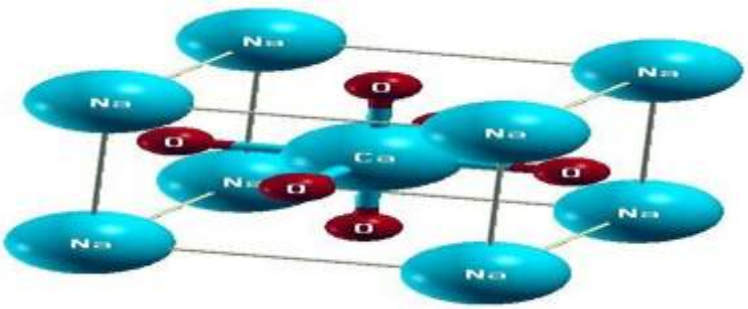

Figure 1: Crystallographic Structure of $NaCaO_3$.

Sodium calcium oxide ($NaCaO_3$) is a ternary oxide with a perovskite-type crystal structure that has attracted interest for its potential in solid oxide fuel cells, catalytic systems, and optoelectronic devices. In its ideal structural form, $NaCaO_3$ typically crystallizes in an orthorhombic or slightly distorted cubic perovskite phase, where Na^+ ions occupy the A-sites, Ca^{2+} ions occupy the B-sites, and oxygen anions are located at the vertices of the CaO_6 octahedral. This arrangement produces a framework of corner-sharing octahedral stabilized by Na^+ cations residing in the larger cuboctahedral voids, as illustrated in Fig. 1. The bonding within $NaCaO_3$ combines ionic and covalent characteristics, with strong ionic interactions between Na^+/Ca^{2+} and O^{2-} and partial covalent contributions within Ca–O bonds, which significantly affect the compound's stability, structural distortions, and physical behavior [7]; [8].

$NaCaO_3$ is particularly notable as an oxide perovskite incorporating both alkali and alkaline earth metals. It crystallizes in the cubic Pm-3m space group, characterized by a three-dimensional framework of corner-linked CaO_6 octahedral. This material is structurally related to a family of Na-based perovskites, including $NaBiO_3$, $NaTiO_3$, $NaBaO_3$, $NaBeO_3$, $NaCoO_3$, $NaTaO_3$, $NaNbO_3$, $NaGeO_3$, $NaSeO_3$, and $NaSiO_3$ [2]; [9]. In related studies, [10] synthesized $CaTiO_3$ nanoparticles via the Pechini chemical method and determined a band gap of 3.4 eV from UV–Vis spectroscopy, confirming its semiconducting behavior. First-principles DFT calculations on $NaCoO_3$, $NaBeO_3$, and $NaBaO_3$ by [9] revealed indirect band gaps, with Co- and Ba-based compounds behaving as wide-bandgap semiconductors, while Be-based perovskites showed insulating properties with mixed ionic–covalent bonding and mechanical stability in the cubic phase, alongside strong UV

absorption. [11] reported that $NaSnCl_3$ and $KSnCl_3$ perovskites exhibit mechanical stability, ductility, and narrow direct band gaps of 1.36 eV and 1.47 eV, respectively, making them promising candidates for photovoltaic and optoelectronic devices. Similarly, DFT-based CASTEP calculations by [2] demonstrated that $NaGeO_3$ and $NaSiO_3$ are semiconductors with narrow indirect band gaps and mechanical stability, with reported lattice constants of 3.79 Å and 3.58 Å, respectively.

Building on these findings, the present study focuses on calculating the electronic band structure, magnetic behavior, and mechanical properties—such as elastic constants and moduli—of $NaCaO_3$. By doing so, it aims to evaluate the compound's stability and assess its suitability for diverse technological applications based on its predicted electronic and mechanical characteristics.

COMPUTATIONAL DETAILS

Computational calculations were carried out using Quantum Espresso [12], a first-principles code based on density functional theory (DFT) [13]. The DFT framework enables accurate simulation of material properties such as electronic structure and mechanical stability by solving the Kohn–Sham equations [14]. The plane-wave pseudopotential method was employed, with the kinetic energy cutoff and k-point mesh carefully optimized to ensure convergence of the results. For the exchange–correlation functional, the Perdew–Burke–Ernzerhof (PBE) approximation [15] was adopted. A Monkhorst–Pack grid of 6×6×6, a kinetic energy cutoff of 95 Ry, and a total energy convergence threshold of 10^{-8} eV/atom were used in the calculations. The valence electron configurations considered were Na ($3s^1$), Ca ($4s^2$), and O ($2s^2 2p^4$).

The $NaCaO_3$ compound crystallizes in the cubic Pm-3m space group, adopting a perovskite structure. The atomic positions within the unit cell are defined by the Wyckoff coordinates: Na at 1a (0, 0, 0), Ca at 1b (½, ½, ½), and O at 3c (0, ½, ½), (½, 0, ½), (½, ½, 0). These Wyckoff positions describe the precise arrangement of atoms within the crystal lattice.

RESULTS AND DISCUSSIONS

Structural and Mechanical properties

The calculated values of the parameters: lattice constant (a) , bulk modulus (B) and pressure derivative (B`) for describing structural properties at ground state are computed and presented in Table 1 for $NaCaO_3$. This was achieved through series of self-consistent calculations. Geometrically the cubic perovskite crystal was optimized.

Table 1: Structural and Mechanical properties of NaCaO3

Properties	Values	Units
a	8.40	Å
B	37.67	Gpa
B`	3.88	
C_{11}	108.22	Gpa
C_{12}	23.90	Gpa
C_{44}	-4.421	Gpa
C_{12}-C_{44}	28.321	Gpa
E	11.288	Gpa
G	5.355	Gpa
B/G	7.032	
N	0.053	

E_f	1.833	eV

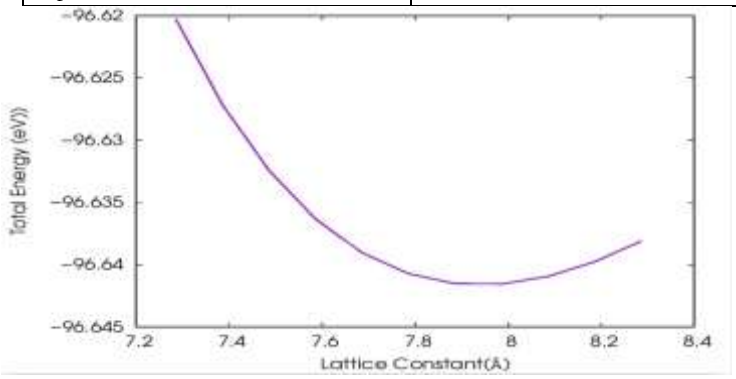

Figure 1: Total energies per unit cell as function of lattice constant for the ferromagnetic (FM) and non-magnetic states.

The elastic constants (C_{11}, C_{12}, C_{44}), shear modulus (G), Young's modulus (E), and Poisson's ratio (v) were calculated and are summarized in table 1. The results reveal that the compound is not mechanically stable, as some of the Born stability criteria—$C_{11} + 2C_{12} > 0$, $C_{11} - C_{12} > 0$, $C_{44} > 0$, and $C_{11} > 0$ [16]; [14] —were not satisfied, with C_{44} yielding a negative value of −4.421 GPa.

To further assess the ductile or brittle nature of $NaCaO_3$, several mechanical indicators were evaluated. These include Poisson's ratio (v), which reflects the lateral strain response; Pugh's ratio (B/G), which measures resistance to fracture; and the Cauchy pressure ($C_{12} - C_{44}$), which provides insights into bonding characteristics [17], [18], [19]. A B/G ratio greater than 1.75 typically indicates ductility, whereas values below this threshold suggest brittleness. Similarly, a positive Cauchy pressure is associated with ductility, while a negative value implies brittleness. In addition, Poisson's ratio offers complementary information, with values approaching 0.5 generally signifying higher ductility.

Lattice Dynamics

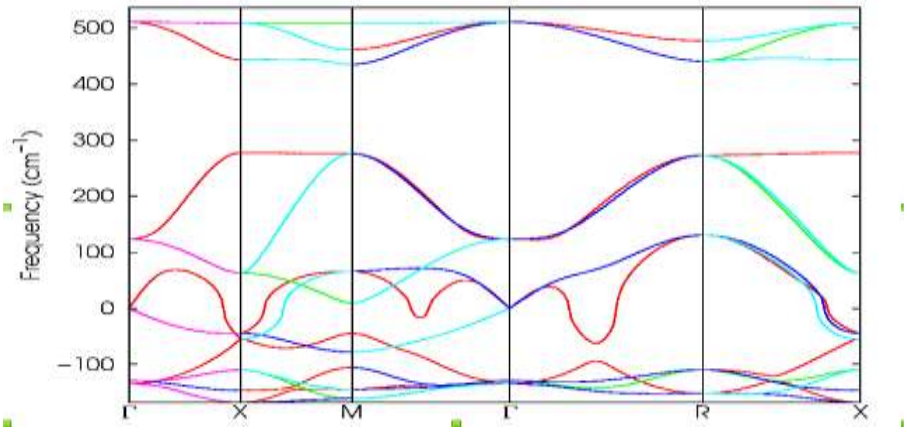

Fig 3: Phonon dispersion of $NaCaO_3$

We investigated the vibrational properties of $NaCaO_3$ by calculating its phonon dispersion curve depicted in Figure 2. Analysis of the phonon dispersion curve reveals dynamic instability in $NaCaO_3$ evidenced by the presences of negative frequencies. With five atoms per unit cell, the perovskite structure exhibits a total of 15 phonon modes. These modes comprise three acoustic branches and 12 optical branches. Notably three optical modes are situated in the low-frequency

region. The highest optical phonon frequency in $NaCaO_3$ approximately 500cm-1

Electronic Property

The electronic characteristics of the $NaCaO_3$ compound have been systematically investigated using Density Functional Theory (DFT) calculations (1).

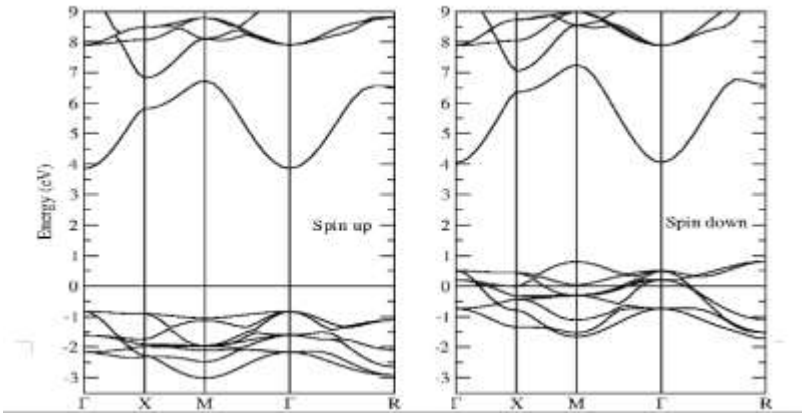

Figure 3: Electronic structure of $NaCaO_3$.

Figure 3 shows the computed electronic band structures. Analysis of the spin-resolved band structures reveals a direct band gap of approximately 4.696 eV in the spin-up configuration, confirming the semiconducting nature of this channel. The PBE functional typically underestimates band gaps due to self-interaction errors and lack of derivative discontinuity. The calculated gap of 4.69 eV for $NaCaO_3$ is usually large for PBE, which may reflect the material's strongly ionic nature or result from numerical artifacts. As PBE is not quantitatively reliable for band gaps, the result should be viewed qualitatively, and more accurate methods like hybrid functionals or GW are recommended for future work. In contrast, the spin-down configuration displays metallic behavior, with bands crossing the Fermi level. This pronounced spin asymmetry demonstrates that $NaCaO_3$, a perovskite oxide, exhibits half-metallicity—a phenomenon in which one spin channel is metallic while the other remains semiconducting [13].

Half-metals are of particular interest for spintronic applications due to their ability to achieve 100% spin polarization at the Fermi level. The half-metallic gap (HMgap) provides further insight into this property, as it quantifies the energy difference between the Fermi level and the nearest edge of either the conduction or valence band [20]. Following the formulation of [21], the HMgap is defined as:

HMgap=min⁡(|Ef−EVMB|,|Ef−ECMB|)(1)HM_{gap} = \min \left(|E_f - E_{VMB}|, |E_f - E_{CMB}|\right) \tag{1}

For $NaCaO_3$, the computed HMgap is 2.669 eV. This parameter is particularly significant, as it reflects the stability and potential device performance of half-metals in practical spintronic environments.

Density of States

The graphs of density of states is shown in figure 4. The density of states (DOS) is plotted against frequency (Hz). The peaks in the plots represent the decomposed orbital contributions to TDOS.

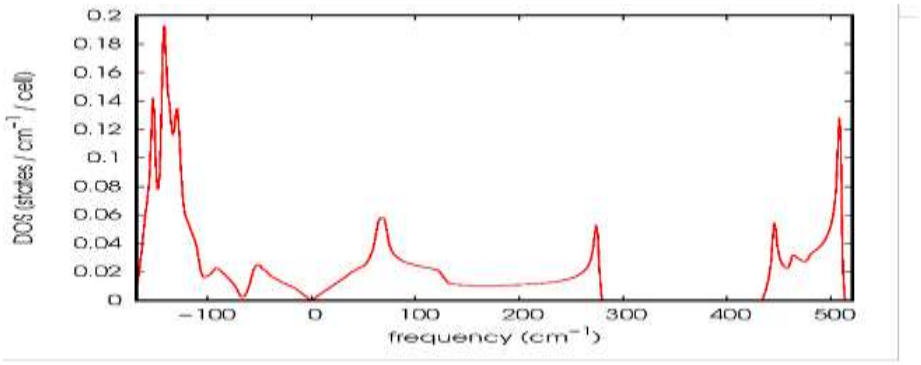

Fig 4: Density of States (DOS) for $NaCaO_3$.

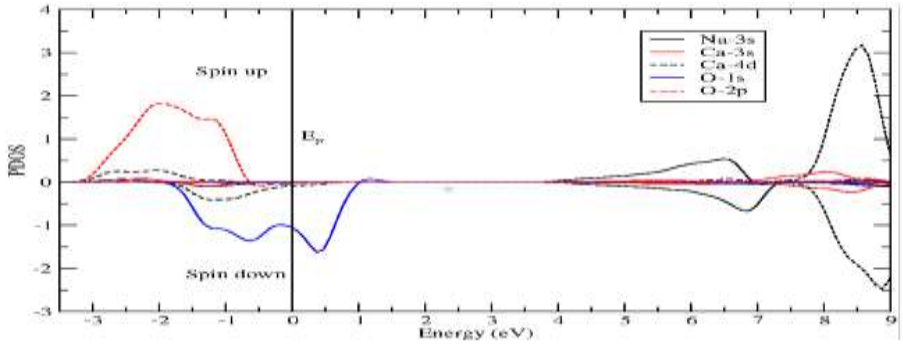

Figure 5: The partial density of states (PDOS) for $NaCaO_3$

The graph of partial density of states (PDOS) is shown in figure 5. The spin-polarized PDOS for $NaCaO_3$ reveals a distinct spin asymmetry near the fermi level. In the down-spin channel, the Ca 4d and 3s-orbitals contribute significantly at the fermi level, indicating metallic behavour and suggesting that these orbitals are involved in delocalized spin-polarized conduction. In contrast, the up-spin channel exhibits a clear separation between the O 2p and Ca 4d states, resulting in a gap across the fermi level. This points to reduced hybridization in the up-spin states and an insulating or semiconducting nature for this spin channel.

The observed Ca O hybridization particularly between Ca 4d and O 2p orbitals, indicates a degree of covalent bonding that influences the electronic structure. The spin imbalance suggests potential half-metallicity, with full spin polarization at the fermi level – an important feature for spintronic applications. These findings underscore the role of orbital hybridization and exchange splitting in determining the materials spin-dependent electronic properties.

CONCLUSION

The structural, mechanical, electronic, and vibrational properties of the $NaCaO_3$ perovskite compound were investigated using density functional theory (DFT) as implemented in the Quantum Espresso software package. The calculations employed the plane-wave pseudopotential method. The electronic band structure indicates that $NaCaO_3$ exhibits half-metallic behavior: the spin-up channel shows semiconducting characteristics with a direct bandgap of 4.69 eV, while the spin-down channel is metallic. Mechanical analysis reveals that the bulk-to-shear modulus ratio is not satisfied due to a negative value of C_{44} (–4.42 GPa), confirming the structure's mechanical instability. The density of states (DOS) analysis further shows that the conduction band is dominated by Ca-4d orbitals, while the valence band is mainly derived from O-2p orbitals. These

findings provide important insights into the intrinsic properties of $NaCaO_3$, underscoring its potential for spintronic and electronic applications. Overall, this research establishes a solid foundation for future experimental and theoretical studies on $NaCaO_3$ and related perovskite systems, thereby advancing the broader understanding of structure–property relationships in functional oxide materials.

REFERENCES

[1] Tayari, F., Teixeira, S. S., Graça, M. P. F., & Nassar, K. T. (2025). A Comprehensive Review of Recent Advances in Perovskite Materials: Electrical, Dielectric, and Magnetic Properties. *Advanced Inorganic Semiconductor Materials, 13*(3), 67–73.

[2] Bibi, N., Usman, M., & Ruyhan, M. (2024). Exploration of Na-based $NaXO_3$ (X = Ge, Si) Oxide Perovskites: A DFT Study. *Computational and Theoretical Chemistry, 1240*, 114842. https://doi.org/10.1016/j.comptc.2023.114842

[3] Frohna, K., & Stranks, S. D. (2019). Photophysics of Organic-Inorganic Hybrid Lead Halide Perovskites. *University of Cambridge. Physics Review, 67*(4), 334–378.

[4] Atta, N. F., Galal, A., & El-Ads, E. H. (2016). Perovskite Nanomaterials – Synthesis, Characterization, and Applications. In L. M. Kustov (Ed.), *Perovskite Materials – Synthesis, Characterisation, Properties, and Applications* (Pp. 107–151). IntechOpen. https://doi.org/10.5772/61900

[5] Asmontas, S., & Mujahid, M. (2023). Perovskite Tandem Solar Cells: A Comprehensive Review. *Center for Physical Sciences and Technology, 45*(3), 234–267.

[6] Daun, T., Mora-Sero, I., & Zhou, Y. (2023). Halide Perovskite Semiconductors: Recent Advances and Future Perspectives. *Advanced Materials Research, 89*(12), 1456–1489.

[7] Lufaso, M. W., & Woodward, P. M. (2001). Prediction of the Crystal Structures of Perovskites Using the Tilt System. *Acta Crystallographica Section B: Structural Science, 57*(6), 725–738

[8] Chen, H., Xu, J., & Zhang, L. (2018). Structural Stability and Electronic Properties of A-Site Substituted Perovskites. *Journal of Materials Chemistry A, 6*(12), 5270–5278.

[9] Ruyhan, M., Usman, M., Bibi, N., Noreen, S., Alqarni, A., Aziz, A., Rahman, S., Aziz, Z., & Abbasi, R. A. (2024). Evaluation of Structural, Electronic, Optical, and Mechanical Properties of Na-Based Oxide Perovskites $NaXO_3$ (X = Co, Be, Ba): A DFT Study. *Materials Today Communications, 39*, 108908. https://doi.org/10.1016/j.mtcomm.2024.108908

[10] Urbano, L. C., Aguilar, C. J., Diosa, J. E., & Vargas, E. M. (2023). Nanoparticles of the Perovskite Structure $CaTiO_3$ System: The Synthesis, Characterization, and Evaluation of its Photocatalytic Capacity to degrade emerging Pollutants. *Nanomaterials, 13*(22), 2967.

[11] Geleta, T. G., Behera, D., Bourri, N., Rivera, V. J. R., & Gonzalo, F. M. (2024). First-Principle Insight into the Study of the Structural, Stability, and Optoelectronic Properties of Alkali-Based Single Halide Perovskite $ZSnCl_3$ (Z = Na/K) Materials for Photovoltaic Applications. *Journal of Computational Chemistry, 45*(30), 2574–2586.

[12] Giannozzi, P., Baroni, S., Bonini, N., Calandra, M., Car, R., Cavazzoni, C., Ceresoli, D., Chiarotti, G. L., Cococcioni, M., Dabo, I., Dal Corso, A., de Gironcoli, S., Fabris, S., Fratesi, G., Gebauer, R., Gerstmann, U., Gougoussis, C., Kokalj, A., Lazzeri, M., ... Wentzcovitch, R. M. (2009). *Quantum Espresso: A Modular and Open-Source Software Project for Quantum Simulations of Materials. Journal of Physics: Condensed Matter, 21*(39), 395502. https://doi.org/10.1088/0953-8984/21/39/395502

[13] Hohenberg, P., & Kohn, W. (1964). Inhomogeneous Electron Gas. *Physical Review, 136*, B864.

[14] Kohn, W., & Sham, L. J. (1965). Self-Consistent Correlation Effects. *Physical Review, 140*, A1133–A1138.

[15] Perdew, J. P., Burke, K., & Ernzerhof, M. (1996). Generalized Gradient Approximation made Simple. *Physical Review Letters, 77*(18), 3865–3868.

[16] Wu, Z., Hao, X., Liu, X., & Meng, J. (2007). Crystal Structure and Elastic Properties of $MgSiO_3$ Perovskite under Pressure: A First-Principles Study. *Physical Review B, 75*(5), 054115. https://doi.org/10.1103/PhysRevB.75.054115

[17] Iyorzor, B. E., Babalola, M. I., Adetuaji, B. T., & Bakare, O. (2018). Effect of Tellurium Concentration on the Structural, Electronic, and Mechanical Properties of Beryllium Sulphide: A DFT Approach. *Materials Research Express, 5*(5), 056517.

[18] Bakare, F. O., Babalola, M. I., & Iyorzor, B. E. (2017). The Role of Alloying Elements on the Structural, Mechanical and Thermodynamic Properties of Al_3X Binary Alloy System (X = Mg, Sc and Zr): First Principles Calculations. *Materials Research Express, 4*(11), 116502.

[19] Pugh, S. F. (1954). Relations between the Elastic Moduli and the Plastic Properties of Polycrystalline Pure Metals. *The London, Edinburgh, and Dublin Philosophical Magazine and Journal of Science, 45*(367), 823–843.

[20] Samara, G. A. (1966). Pressure and Temperature Dependences of the Dielectric Properties of the Perovskites $BaTiO_3$ and $SrTiO_3$. *Physical Review, 151*, 378–386.

[21] Sin'ko, G. V., & Smirnov, N. A. (2002). *Ab initio* Calculations of Elastic Constants and Thermodynamic Properties of Bcc, Fcc, and Hcp Al Crystals Under Pressure. *Journal of Physics: Condensed Matter, 14*, 6989–7005.

[22] Vanderbilt, D. (1990). Soft Self-Consistent Pseudopotentials in a generalized eigenvalue formalism. *Physical Review B, 41*(11), 7892–7895.

[23] Fan, L., Chen, F., & Chen, Z. Q. (2019). Electronic Structure and Magnetic Properties of Double Perovskite La_2Femno_6 from First-Principles Calculations. *Journal of Magnetism and Magnetic Materials, 478*, 264–270. https://doi.org/10.1016/j.jmmm.2019.01.044

[24] Du, J., Dong, S., Lu, Y. L., Zhao, H., Feng, L., & Wang, L. Y. (2017). Structural, Electronic and Magnetic Properties of Double Perovskite La_2MnNiO_6: A First-Principles Study. *Journal of Magnetism and Magnetic Materials, 428*, 250–256. https://doi.org/10.1016/j.jmmm.2016.12.033